

Theoretical Study of the $C_6H_5NH_2 + CH_3$ Reaction by the Density Functional Theory DFT/M06-2X/6-311++G(3df,2p)

Tran Duc Chien, Nguyen Duc Trung, Tien V. Pham*

Hanoi University of Science and Technology, Hanoi, Vietnam

*Email: tien.phamvan@hust.edu.vn

Abstract

The mechanism of the reaction between Aniline compound ($C_6H_5NH_2$) and Methyl radical (CH_3) has been studied by using the density functional theory DFT/M06-2X in conjunction with the 6-311++G(3df,2p) basis set for both optimization and single-point energy calculations. The calculated results indicate that the mechanism of the $CH_3 + C_6H_5NH_2$ reaction can occur in two different directions, namely, H-atom abstraction and addition. As a result, 13 various products have been created from this reaction; in which, P1 ($C_6H_5NH + CH_4$) is the most thermodynamically stable product and the reaction path leading to this product is also the most energetically and kinetically favorable channel. The calculated thermodynamic properties for all reaction channels in the $C_6H_5NH_2 + CH_3$ system are in good agreement with the literature values derived from the Active Thermochemical Tables. The T1 diagnostics and the spin contamination effect of all species involved have insignificant multireference character and can be ignored.

Keywords: DFT, CH_3 , $C_6H_5NH_2$, M06-2X, 6-311++(3df,2p).

1. Introduction

Aniline ($C_6H_5NH_2$), consisting of an amino group ($-NH_2$) attached to a phenyl group ($-C_6H_5$), is considered the simplest aromatic amine. It is an important source material in the chemical industry in the manufacture of precursors of dyes, polyurethane, pigments, paints, fabrics, rubbers, explosives, drugs, crop protection agents, and other chemicals. Aniline can enter the atmosphere during its manufacture and usage with a concentration of up to tens of parts per trillion by volume [1]. It is worth mentioning that aniline is classified as a potentially hazardous organic NH_x -containing compound ($x = 1$ and 2) due to its high toxicity [2] and biochemical permanence [3]. The general population is known to be ubiquitously exposed to aniline. Thus, assessment of aniline exposure is of both occupational and environmental relevance. Knowledge on human metabolism of aniline is still scarce. Mechanisms by which aniline exposure elicits splenotoxicity, especially a tumorigenic response, are not well-understood. It is known that aniline exposure causes oxidative damage to the spleen [4]. In contrast to (oxygenated) hydrocarbons, the atmospheric oxidation of amines could produce N-centered radicals, forming highly carcinogenic nitrosamines and nitramines [5] through bimolecular reactions with NO and NO_2 , respectively. This is because these N-centered radicals often react slowly with O_2 molecules; consequently, they will possibly be removed by other atmospheric trace compounds, for example, NO and NO_2 [6]. Therefore, the comprehensive understanding of the sinks and lifetime of amines in the troposphere is of utmost

relevance to environment and risk concerns the use of amines [7].

Methyl radical (CH_3), an important agent in fossil fuel combustion, is an isoelectronic species which appears remarkably in the troposphere. Due to its high reactivity, the CH_3 radical is considered to be one of the detergents of the troposphere, which can react with almost all air pollutants including the aniline compound [8,9]. The reaction between aniline and the CH_3 free radical is thought to be possible in the troposphere with a very high reaction probability because they are both present in this environment as mentioned above. Therefore, finding the mechanism and kinetics for the reaction of aniline with the methyl radical has an important role to understand how aniline is converted into other chemical compounds by the CH_3 radicals in the troposphere.

To our knowledge, no studies have been devoted to the reaction of $C_6H_5NH_2$ with CH_3 . It was found that the chemistry of aniline is a prototype for complex nitrogen-containing compounds of potential relevance to combustion applications. Therefore, the current study focuses on investigating the possibility of explaining the behavior of aniline through the application of quantum mechanical methods. It is anticipated that modern technology will lead to a greater understanding of the associated chemical mechanisms and open the route for future studies of other aromatic amines. In order to have a more comprehensive insight of the title reaction, its mechanism is going to be examined thoroughly within this study based on the structures of all species

involved which were optimized at the M06-2X/6-311++G(3df,2p) level of theory. Here the mechanism of 4 addition reactions and 4 hydrogen abstractions, either from the NH₂ group or the benzene ring via CH₃[•] radicals have been carefully considered. The higher level of study such as CCSD(T)/CBS will be examined for this system in our next study to support kinetic treatment.

2. Computational Methods

The potential energy surface (PES) of the C₆H₅NH₂ + CH₃[•] bimolecular reaction has been characterized by quantum chemical calculations using the density functional theory (DFT) with the common M06-2X [10,11] functional in conjunction with the 6-311++G(3df,2p) basis set. In this work, the geometries optimized by the M06-2X/6-311++G(3df,2p) method were utilized for the establishment of the potential energy surface (PES). The correlative parameters including vibrational frequencies, moments of inertia, and zero-point vibrational energies (ZPVE) were obtained at the same method. All species in the system were classified based on their vibrational analysis, in which the local minima such as reactants, intermediates, and products have all positive frequencies, while a transition state must contain an imaginary frequency. The intrinsic reaction coordinate (IRC) [12] approach was utilized

to identify the validity of transition states. The M06-2X/6-311++G(3df,2p) relative energies of all points on the PES were then refined by the single-point energy calculations using the M06-2X/6-311++G(3df,2p) level of theory. The ZPVE values were scaled by a factor of 0.971 [13]; hence, the energy values of all species involved have been calculated by the equation: $E = (E_{HF} \times 2625.45 + ZPVE \times 0.971)$ (kJ/mol). The value of E was then divided by 4.184 to convert from the kJ/mol unit into the unit of kcal/mol. Because the single-point energy E_{HF} holds the atomic unit (a.u.), its value must be multiplied by a 2625.45 to convert a.u. into kJ/mol. In order to optimize a substance, its structure was originally built in the Gaussview 06 software program to get a reaction coordinate in Cartesian coordinates (CCs); these CCs were then put into the Gaussian 16 software package [14] to carry out optimization processes and compute single-point energy. The single-point energies of all species were then used to compute the standard enthalpy changes for the reaction channels in the C₆H₅NH₂ + CH₃ system by using the M06-2X/6-311++G(3df,2p) method. For comparison, the CCSD(T)/6-31+G(d) level was also utilized in this calculation. All computations were implemented by the high-speed server of the National Center for High-performance Computing (NCHC) in Taiwan.

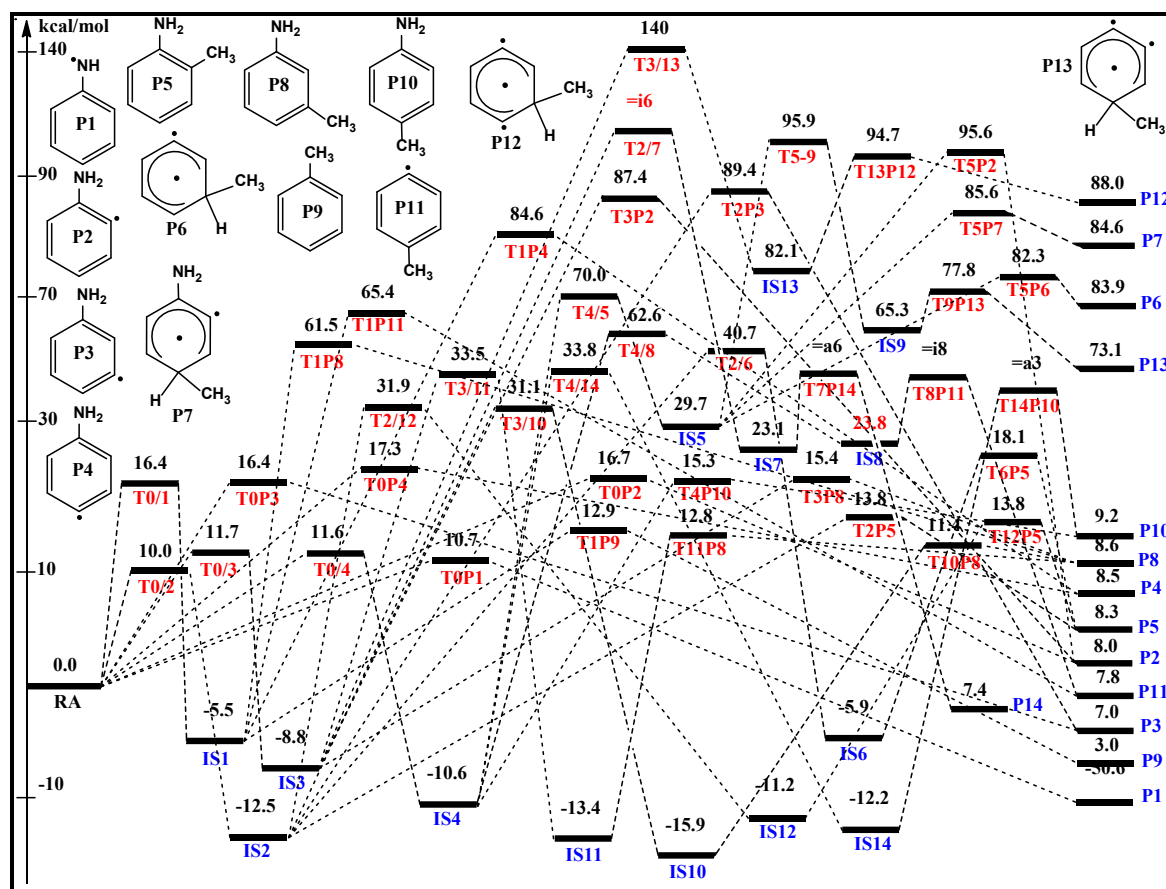


Fig. 1. The potential energy surface of the C₆H₅NH₂ + CH₃[•] reaction calculated at the M06-2X/6-311++G(3df,2p) + ZPVE level of theory. (Energies are in units of kcal/mol).

3. Results and Discussions

3.1. Analysis of the Potential Energy Surface

As stated above, all species involved in the title reaction were optimized at the M06-2X/6-311++G(3df,2p) level of theory. The detailed mechanism of the system describing all reaction channels is graphically plotted in Fig. 1. Some main intermediate and transition states are displayed in Fig. 2 and 3, respectively. From Fig. 1, it is easy to see that many bimolecular products including four CH₄-containing products (P1 – P4), four H-containing products (P5, P7, P8, P10), two NH₂-containing products (P6, P9), and four NH₃-containing products (P11 – P13) can be formed when CH₃ attacks aniline compound by the abstraction or addition directions.

Among those products, the four CH₄-containing products, namely P1 (C₆H₅NH + CH₄), P2 (o-C₆H₄NH₂ + CH₄), P3 (m-C₆H₄NH₂ + CH₄), and P4 (p-C₆H₄NH₂ + CH₄), were generated by the H-abstraction channels going via the transition states TOP1, TOP2, TOP3, and TOP4 located at the energy levels of 10.7, 16.7, 16.4, and 17.3 kcal/mol, respectively, above the reactants, while other products were created by the addition channels going through four transition states T0/1, T0/2, T0/3, and T0/4 before transferring to four intermediate states IS1, IS2, IS3, and IS4, respectively, as shown in Fig. 1. The TOP1 geometric structure optimized at the M06-2X method shows that a hydrogen atom is abstracting from the NH₂ group of aniline at the distance of 1.2 Å and is coming to the CH₃ carbon atom at the loose bond length of 1.4 Å (see Fig. 3). This abstraction is characterized by an imaginary frequency of ~1740i cm⁻¹ shown in the TOP1 harmonic oscillator modes. The three transition states TOP2, TOP3, and TOP4 display the same trend of H-abstraction processes from the positions of ortho, meta, and para of aniline compound. The breaking bond length C – H and the forming bond length CH₃ – H in these transition states are found to be about 1.4 and 1.3 Å, respectively. It is worth noting that the abstraction reaction channel generating to P1 is the most energetically and kinetically favorable channel and it is also a unique exothermic reaction path with the energy released by about 50.6 kcal/mol. All three remaining separation reaction paths forming the P2, P3, and P4 products are endothermic processes with the energy absorbed ranging from 7 to 8.5 kcal/mol.

It can be seen that the first addition channel leading to IS1 is not convenient in energy compared to the remaining three addition channels resulting in IS2, IS3, and IS4 because the T0/1 energy barrier is about 5 – 6 kcal/mol higher than that of T0/2, T0/3, and T0/4, *cf.* Fig. 1. It can be said that the intermediates IS2, IS3, and IS4 whose structures are shown in Fig. 2 have the same formation probability because the relative

energies of T0/2, T0/3, and T0/4 are similar, being 10, 11.7, and 11.6 kcal/mol, respectively.

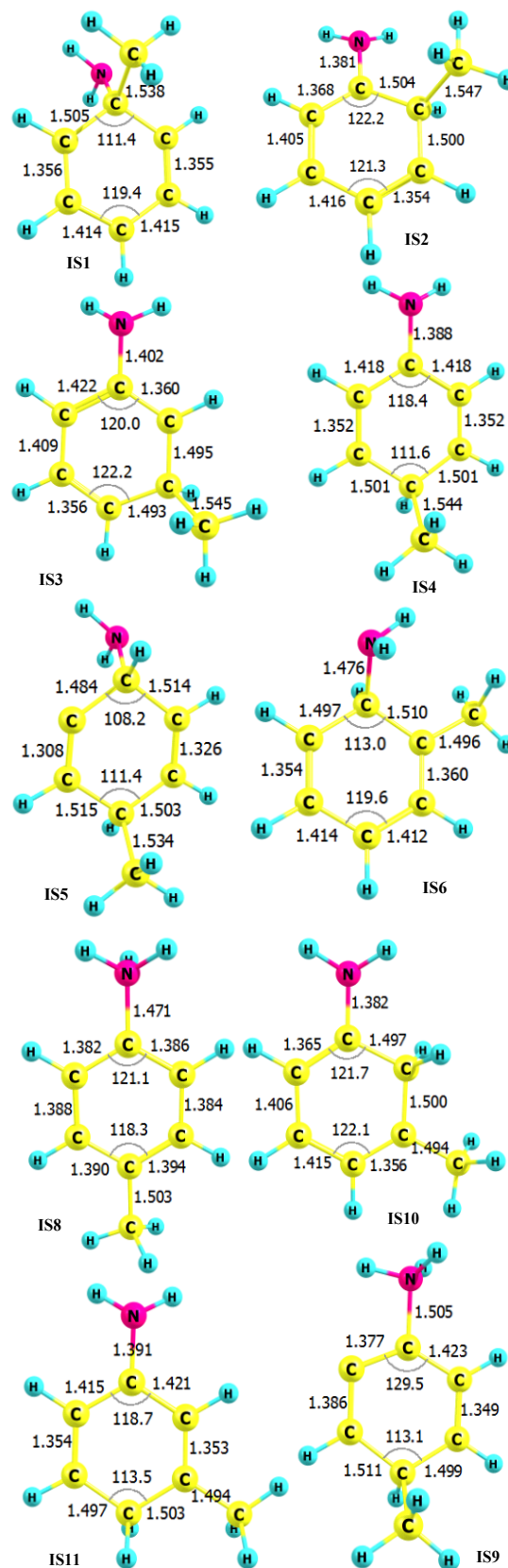


Fig. 2. Some main intermediate states on the PES of the C₆H₅ + CH₃ reaction.

From the four intermediate states, IS1 – IS4, many isomers and/or final products, P5 – P14, can be formed via the isomerization and/or the dissociation processes, in which the products P4, P8, P9, and P11 can be directly created from IS1 by the CH₄-loss, NH₃-loss, and NH₂-loss processes via the transition state T1P4, T1P8, T1P9, and T1P11 located at positions of 86.4, 61.5, 12.9, and 65.4 kcal/mol, respectively, on the PES. Clearly, the P9(C₆H₅CH₃ + NH₂) product is more easily created than the other 3 ones. This product is also relatively stable compared to the others, its relative energy is only 3.0 kcal/mol above the entry point. The structure of the T1P9 transition state holding an imaginary frequency of 592i cm⁻¹ describes the NH₂-abstraction process at a distance of around 2.0 Å, *cf.* Fig. 3. Due to the barrier heights of T1P4, T1P8, and T1P11, the products P4, P8, and P11 are predicted to be extremely difficult to form under normal conditions. Unlike the above products, the P3 (C₆H₄NH₂ + CH₄) and P5 (o-methylaniline + H) products can be formed directly or indirectly from the IS2 intermediate state as can be seen in Fig. 1, in which the P3 product was generated when IS2 passed through the T2P3 transition state (TS). However, this TS owns a so high energy barrier, being about 89 kcal/mol; therefore, it can be said that the IS2 → T2P3 → P3 channel has almost no contribution to the P3 formation. Instead, the product P3 is mainly formed by the RA → T0P3 → P3 channel as mentioned above, where RA is known to be the reactants (C₆H₅NH₂ + CH₃), also called the entrance point. Meanwhile, product P5 is not only created directly but also indirectly from the IS2 intermediate. The direct channel goes through the T2P5 saddle point, while two indirect channels proceed via the transition states T2/6 and T6P5 or T2/12 and T12P5. In terms of energy, the IS2 → T2P5 → P5 channel is more convenient than the two remaining channels because the energy of the T2P5 is much lower than that of the T2/6 and the T2/12 (13.8 vs. 40.7 and 31.9 kcal/mol). Thus, the former channel will be considered for the kinetic calculation rather than the two later channels. Structurally, the T2P5 geometry displays an H-abstraction process with the breaking bond length of 1.77 Å, *cf.* Fig. 3, which is identified by an imaginary frequency of 901i cm⁻¹. The bimolecular product P5 containing a hydrogen atom and an o-methyl-aniline holds an energy level of 8.3 kcal/mol above the entry point. From the IS3 intermediate, three final products P2, P8, and P12 have been established. The P2 (C₆H₅NH₂ + CH₄) is the product of the simultaneous separation of H at the ortho position and CH₃ at the para position from the structure of IS3. The abstraction distances recorded at the T3P2 geometry are 1.3 Å for C – H and 2.2 Å for C – CH₃ corresponding to an unreal harmonic oscillation frequency of ~1495i cm⁻¹. Then the two free radicals immediately combine to form the CH₄ molecular which is a part of the P2 product. The P8 (m-toluidine + H) product has been achieved by three

different pathways, known as IS3 → T3P8 → P8, IS3 → T3/10 → IS10 → T10P8 → P8, and IS3 → T3/11 → IS11 → T11P8 → P8; where the first path goes directly from IS3 to P8 via the T3P8 saddle point. Whereas the second and third paths are the indirect reaction channels owing to they must isomerize to IS10 and IS11 before settling down at the P8 product. The first one is an H-abstraction process out of the ortho position of IS3 with the C – H bond breaking of 1.74 Å, *cf.* Fig. 3, which was realized by a 1023i cm⁻¹ negative frequency. The energy level of the T3P8 saddle point and the P8 product are only about 15.4 and 8.6 kcal/mol, respectively, showing that the two endothermic reaction channels, namely RA → T0/2 (10.0) → IS2 (-12.5) → T2P5 (13.8) → P5 (8.3 kcal/mol) and RA → T0/3 (11.7) → IS3 (-8.8) → T3P8 (15.4) → P8 (8.6 kcal/mol), are competitive with each other in the formation of the P5 and P8 products. Compared with the first path, the second and third paths are less favorable in energy due to the energy barriers of the T3/10 and T3/11 transition states which they must come over are rather high, being about 40 and 42 kcal/mol, respectively. Hence, the P8 product was predicted to be formed by the reaction channel going via the T3P8 transition state rather than the other ones. The last of the three products created from the IS3 intermediate, namely P12 (C₆H₄CH₃ + NH₃), is extremely difficult to appear in the number of products of the title reaction due to the first-order saddle point T3/13, the highest TS on the PES, lying on the channel leading to this product owns a so high energy level, being ~ 149 kcal/mol. Moreover, it is not difficult to realize that the P12 product is the most thermodynamically unstable in comparison with the others and the reaction path producing this product needs to absorb about 88 kcal/mol energy, which is not suitable for any conditions of combustion chemistry and atmospheric chemistry.

From the intermediate state IS4 (4-hydrogen-p-toluidine, *cf.* Fig. 2), three isomers (IS5, IS8, IS14) and the P10 final product can be directly produced by the isomerization and decomposition processes of IS4 → IS5, IS4 → IS8, IS4 → IS14, and IS4 → P10 going via the transition states T4/5, T4/8, T4/14, and T4P10 with relative energies of 70, 62.6, 33.8, and 15.3 kcal/mol, respectively. After forming the IS14 isomer (3-hydrogen-p-toluidine, -12.2 kcal/mol), the product P10 (p-toluidine + H) was also created by an H-loss process via the T14P10 transition state located at the energy of 14.2 kcal/mol above the reactants. The T14P10 transition state contains only one imaginary frequency of ~879i cm⁻¹ corresponding to the removing of the H atom at the meta position out of the IS14 structure with the bond breaking C(3) – H recorded at the T14P10 transition state as 1.8 Å. Thus, it can be seen that from IS4 the P10 product can be produced either by the direct channel IS4 → T4P10 → P10 or by the indirect channel IS4 → T4/14 → IS14

→ T14P10 → P10. The second channel must go over the very high TS, T4/14 (33.8 kcal/mol), whereas the T4P10 energy level on the first channel is only 15.3 kcal/mol; therefore, the first path is made easier than the second one. Furthermore, in terms of energy, the first channel together with the two other channels IS2 → T2P5 → P5 and IS3 → T3P8 → P8 are the reaction paths that have the same energy level, *cf.* Fig. 1.

The IS5 intermediate created was the result of the isomerization process between the IS4 and IS5 isomers via the T4/5 saddle point; however, the IS5 is not stable due to its relative energy is rather high, being nearly 30 kcal/mol. This isomer then decomposes to the products P2, P6, P7 or continues isomerizing to the IS9 intermediate before stopping at the final product P13. Accordingly, the P2 product was generated as IS5 passed over the T5P2 point at the level of 95.6 kcal/mol; this is a simultaneous abstraction of H atom and CH₃ radical at the (1) and (4) positions of the IS5 structure with the C(1) – H and C(4) – CH₃ bond lengths of 1.36 and 2.1 Å, respectively. Compared to the direct abstraction channel RA → T0P2 → P2, the reaction path going via the IS5 intermediate and the T5P2 transition state consumes much more energy; hence, this channel should not be considered for the later kinetic calculation part. The P6 and P7 products were also created by the dissociations of IS5 via T5P6 and T5P7, respectively. If the T5P6 displays an NH₂-loss process with a loose C – NH₂ distance of 2.4 Å and an imaginary frequency of 282i cm⁻¹, the T5P7 saddle point shows an H-loss procedure identified by a 2.15 Å weak bond length of C – H ($\nu_i = 517i$ cm⁻¹). Nevertheless, both the T5P6 and T5P7 transition states hold the high energy level of 85.2 and 85.6 kcal/mol, respectively, and both the products P6 (83.9 kcal/mol) and P7 (84.6 kcal/mol) are also unstable in thermodynamics; therefore, those products are almost not visible in the normal condition. They may occur in regions of elevated temperatures and pressures because under these conditions they can be energized enough to overcome the high energy barriers. Similar to the P6 and P7 products, the P13 product holding NH₃ and C₆H₄CH₃ is also not easy to appear when the methyl radical and aniline compound collide with each other due to the reaction path going from the starting point (CH₃ + C₆H₅NH₂) to P13 has to proceed via three first-order saddle points T4/5, T5/9, and T9P13 whose the relative energy values are too high in comparison with the lowest transition state T0P1; those values are larger than the T0P1 energy value approximately 60 – 85 kcal/mol calculated at the M06-2X/6-311++G(3df,2p) level of theory. It can be seen that this bimolecular product is less stable in thermodynamics because it is the product of a strongly endothermic process with an absorbed energy level of 73 kcal/mol. Last but not least, the IS8 (23.8 kcal/mol) was created by the isomerization process of IS4 via the

T4/8 (62.6 kcal/mol). Because it is energetically unstable, this isomer then rapidly converts to the P11 product via T8P11 (33.6 kcal/mol). The channel going via IS8 will therefore not used for kinetic prediction.

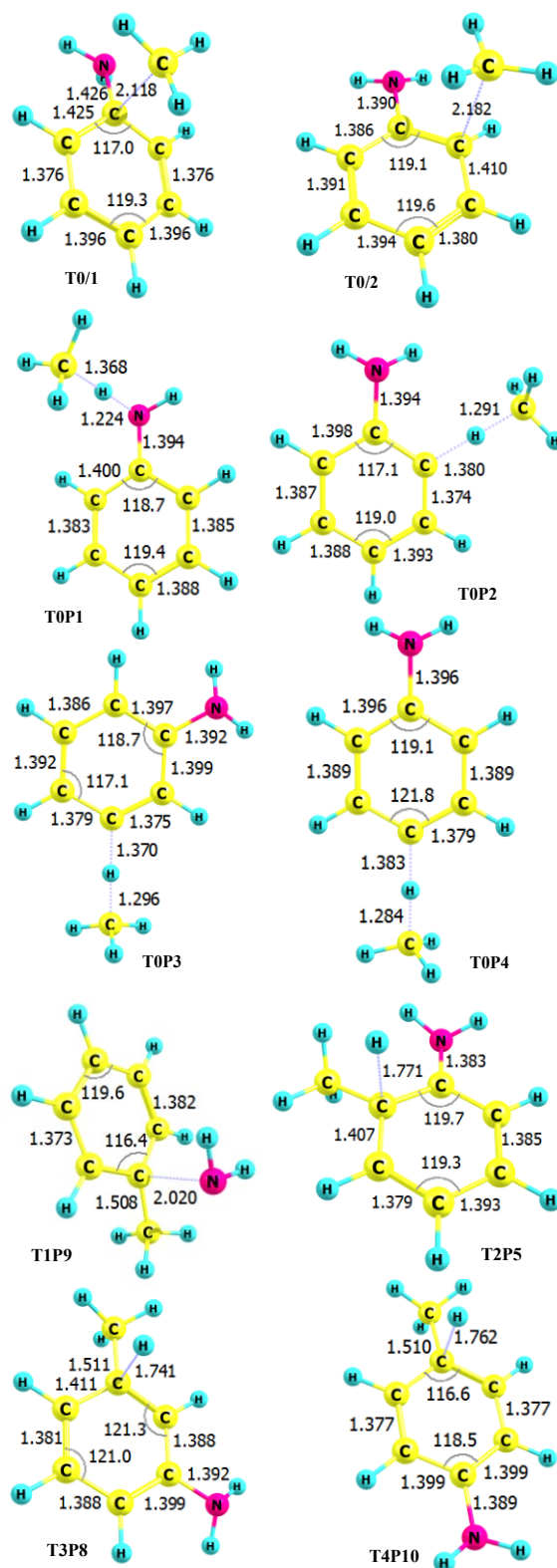


Fig. 3. Some main transition states on the PES of the C₆H₅NH₂ + CH₃ reaction.

3.2. Thermochemical Properties

To access the accuracy of such calculations, the calculated thermodynamic properties (ΔH_{298}^0) for all reaction channels in the $C_6H_5NH_2 + CH_3$ system were presented in Table 1 and compared to experimental data derived from the Active Thermochemical Tables (ATcT), from NIST, and from reference [15]. As easily seen in Table 1, the calculated values are in good agreement with the literature values within their uncertainties (e.g., the maximum difference between our numbers and ATcT is less than 2.0 kcal/mol). Such good agreements on the computed thermodynamic parameters reveal that the M06-2X method in conjunction with the Pople 6-311++G(3df,2p) basis set is a reasonably suitable choice for the title reaction. Moreover, in this calculation, the CCSD(T)/6-31+G(d) level of theory has also been employed to predict the standard enthalpy change for all of the reaction paths. Because the CCSD(T)/6-31+G(d) method is more expensive than the M06-2X/6-311++G(3df,2p) one, so it is the best choice to select the latter method if the latter results are not far from the former data. It can be seen from Table 1 that the values computed at the M06-2X/6-311++G(3df,2p) level are in close with those predicted at the CCSD(T)/6-31+G(d) level except for the values of the $C_6H_5NH_2 + CH_3 \rightarrow P6$ ($C_6H_4(H)CH_3 + NH_2$) and $C_6H_5NH_2 + CH_3 \rightarrow P7$ ($H(CH_3)C_6H_3NH_2 + H$) reaction channels. The deviation between the first and second methods for the P6 channel is 8.69 kcal/mol, while the difference for the P7 channel is up to 9.44 kcal/mol. However, the experimental values for these two reaction paths have not been published yet; hence, there is no basis for

asserting which method is more correct than the other in this case.

For the first reaction, $C_6H_5NH_2 + CH_3 \rightarrow P1$ ($C_6H_5NH + CH_4$), is the most energetically and thermodynamically favorable channel as mentioned above. The enthalpy change for this path is therefore the smallest compared to all other pathways, which is -51.72 or -53.64 kcal/mol calculated at the methods M06-2X or CCSD(T), respectively. The deviation between them is about 2 kcal/mol. Whereas, the experimental value for this channel is -53.54 ± 0.08 kcal/mol which agrees well with the CCSD(T) value. The 2nd, 3rd, and 4th reaction pathways yield three products, namely, P2: *o*- $C_6H_4NH_2 + CH_4$, P3: *m*- $C_6H_4NH_2 + CH_4$ and P4: *p*- $C_6H_4NH_2 + CH_4$, which are isomers of each other. The enthalpy changes for them are also roughly equivalent to one another, being 7.85, 6.82, and 8.33 kcal/mol at the M06-2X method and 8.92, 9.84, and 11.16 kcal/mol at the CCSD(T) level. The laboratory values for those channels were recorded to lie between the M06-2X and CCSD(T) data, which are 8.45 ± 0.32 , 7.56 ± 0.86 , and 9.78 ± 1.0 kcal/mol for the 2nd, 3rd, and 4th reaction paths, respectively.

The next three pathways which also lead to the isomer products P5 (*o*- $CH_3-C_6H_4NH_2 + H$), P8 (*m*- $CH_3-C_6H_4NH_2 + H$), and P10 (*p*- $CH_3-C_6H_4NH_2 + H$) have the same enthalpy changes for both the M06-2X and CCSD(T) approach, being (8.13, 8.69, 8.79) and (4.15, 4.40, 4.37) kcal/mol, respectively. The measured values seem to favor the M06-2X method rather than the CCSD(T) method, however, as can be seen in Table 1.

Table 1. The standard enthalpy changes (kcal/mol) of the thirteen reaction channels in the $C_6H_5NH_2 + CH_3$ system calculated at the M06-2X/6-311++G(3df,2p) level of theory in comparison with those computed at the CCSD(T)/6-31+G(d) level and experimental data.

Reaction channels	M06-2X/6-311++G(3df,2p)	CCSD(T)/6-31+G(d)	Expt.*
$C_6H_5NH_2 + CH_3 \rightarrow P1$ ($C_6H_5NH + CH_4$)	-51.72	-52.64	-53.54 ± 0.08
$C_6H_5NH_2 + CH_3 \rightarrow P2$ (<i>o</i> - $C_6H_4NH_2 + CH_4$)	7.85	8.92	8.45 ± 0.32
$C_6H_5NH_2 + CH_3 \rightarrow P3$ (<i>m</i> - $C_6H_4NH_2 + CH_4$)	6.82	9.84	7.56 ± 0.86
$C_6H_5NH_2 + CH_3 \rightarrow P4$ (<i>p</i> - $C_6H_4NH_2 + CH_4$)	8.33	11.16	9.78 ± 1.0
$C_6H_5NH_2 + CH_3 \rightarrow P5$ (<i>o</i> - $CH_3-C_6H_4NH_2 + H$)	8.13	4.15	8.59 ± 0.5
$C_6H_5NH_2 + CH_3 \rightarrow P6$ ($C_6H_4(H)CH_3 + NH_2$)	84.10	75.41	N/A
$C_6H_5NH_2 + CH_3 \rightarrow P7$ ($H(CH_3)C_6H_3NH_2 + H$)	84.81	75.37	N/A
$C_6H_5NH_2 + CH_3 \rightarrow P8$ (<i>m</i> - $CH_3-C_6H_4NH_2 + H$)	8.69	4.40	7.23 ± 1.5
$C_6H_5NH_2 + CH_3 \rightarrow P9$ ($C_6H_5CH_3 + NH_2$)	3.07	-0.97	0.72 ± 0.88
$C_6H_5NH_2 + CH_3 \rightarrow P10$ (<i>p</i> - $CH_3-C_6H_4NH_2 + H$)	8.79	4.37	6.3 ± 1.2
$C_6H_5NH_2 + CH_3 \rightarrow P11$ ($C_6H_4CH_3 + NH_3$)	7.83	7.65	7.54 ± 0.22
$C_6H_5NH_2 + CH_3 \rightarrow P12$ (<i>m</i> - $H(CH_3)-C_6H_3 + NH_3$)	88.18	88.18	88.12 ± 0.15
$C_6H_5NH_2 + CH_3 \rightarrow P13$ (<i>p</i> - $H(CH_3)-C_6H_3 + NH_3$)	73.38	72.17	72.48 ± 0.15

*derived from ATcT (<https://atct.anl.gov/Thermochemical%20Data/version%201.118/index.php>), from NIST (webbook.nist.gov), and from reference 15.

Unlike the above-mentioned reaction channels, the $C_6H_5NH_2 + CH_3 \rightarrow P9$ ($C_6H_5CH_3 + NH_2$) reaction seems to be the swapping between the CH_3 and NH_2 radicals; the enthalpy change of this channel is thus relatively small, which is just over 3.0 kcal/mol at the M06-2X level and is nearly -1.0 kcal/mol at the CCSD(T) method, while the experimental value was reported as 0.72 ± 0.88 kcal/mol. The last three channels known as $C_6H_5NH_2 + CH_3 \rightarrow P11$ ($C_6H_4CH_3 + NH_3$), $C_6H_5NH_2 + CH_3 \rightarrow P12$ (m-H(CH₃)-C₆H₃ + NH₃), and $C_6H_5NH_2 + CH_3 \rightarrow P13$ (p-H(CH₃)-C₆H₃ + NH₃) are the NH₃-loss processes resulting in the isomer products of C₆H₄CH₃. Among those reaction channels, the first one has the lowest enthalpy change which is 7.83, 7.65, and 7.54 ± 0.22 kcal/mol at the M06-2X, CCSD(T), and experimental methods, respectively, indicating that the P11 product is more favorable than the two remaining ones, which is suitable with the above-analyzed energy section. The two reaction paths forming P12 and P13 hold the very high values of ΔH_{298}^0 , being nearly 88 and 73 kcal/mol, respectively, showing that these two products may not occur in the normal conditions of temperatures and pressures. This statement is completely consistent with the conclusion in the energy analysis of the reactions on the PES. Another point should also be noted that the enthalpy levels of each channel in those three channels are the same for both methods M06-2X and CCSD(T) as well as the laboratory measurement. This once again confirms that the method used in the present study is workable and reliable.

3.3. Diagnostic and Spin Contamination Analysis

To ascertain the reliability of our calculated results, the T1 diagnostic analysis was implemented at the M06-2X/6-311++G(3df,2p) method to measure approximately the multireference character in the wave function. The results for the reactants, products, intermediate states, and main transition states of the title reaction are summarized in Table 2. The calculated values show that the T1 diagnostics of all species do not have significant multireference character because all the values for singlet-state species are less than 0.02 (the threshold for T1 diagnostic of a closed-shell species was reported as 0.02), while all the values for doublet-state species do not exceed the number of 0.045 (the threshold for T1 diagnostic of an open-shell species was known to be ~0.045) except for the two fragments of P12 and P13, m-H(CH₃)-C₆H₃ and p-H(CH₃)-C₆H₃, have large T1 diagnostics, being 0.051 and 0.048, respectively, at the M06-2X/6-311++G(3df,2p) level, leading to inaccurate in energy for these two species. However, the P12 and P13 products were predicted to be not important to the $C_6H_5NH_2 + CH_3$ system; therefore it can be said that the single-reference methods can be reliably employed in the present study. Moreover, it can be seen from Table 2, the spin contamination values $\langle S^2 \rangle$ for species in the singlet states are 0.0 while those for species in the doublet states are round 0.76, indicating that the spin contamination effect on the estimation of activation barriers and the structures of all species is negligible.

Table 2. The results of T1 diagnostic analysis and spin contamination $\langle S^2 \rangle$ for most species on the PES of the $C_6H_5NH_2 + CH_3$ system carried out at the M06-2X/6-311++G(3df,2p) level of theory.

Species	T1 / $\langle S^2 \rangle$	Species	T1 / $\langle S^2 \rangle$	Species	T1 / $\langle S^2 \rangle$
C ₆ H ₅ NH ₂ (singlet)	0.012 / 0.0	T0/1 (doublet)	0.021 / 0.76	C ₆ H ₅ NH	0.032 / 0.71
CH ₃ (doublet)	0.016 / 0.75	T0/2 (doublet)	0.020 / 0.71	o-C ₆ H ₄ NH ₂	0.019 / 0.75
IS1 (doublet)	0.021 / 0.74	T0/3 (doublet)	0.022 / 0.76	m-C ₆ H ₄ NH ₂	0.039 / 0.76
IS2 (doublet)	0.018 / 0.77	T0/4 (doublet)	0.035 / 0.74	p-C ₆ H ₄ NH ₂	0.039 / 0.74
IS3 (doublet)	0.028 / 0.73	T0P1 (doublet)	0.021 / 0.75	o-CH ₃ -C ₆ H ₄ NH ₂	0.015 / 0.0
IS4 (doublet)	0.021 / 0.76	T0P2 (doublet)	0.017 / 0.77	C ₆ H ₄ (H)CH ₃	0.014 / 0.0
IS5 (doublet)	0.021 / 0.75	T0P3 (doublet)	0.036 / 0.75	H(CH ₃)C ₆ H ₃ NH ₂	0.019 / 0.0
IS6 (doublet)	0.017 / 0.76	T0P4 (doublet)	0.033 / 0.76	m-CH ₃ -C ₆ H ₄ NH ₂	0.012 / 0.0
IS8 (doublet)	0.012 / 0.77	T1P9 (doublet)	0.023 / 0.73	C ₆ H ₅ CH ₃ (singlet)	0.011 / 0.0
IS9 (doublet)	0.026 / 0.78	T2P5 (doublet)	0.031 / 0.76	p-CH ₃ -C ₆ H ₄ NH ₂	0.012 / 0.0
IS10 (doublet)	0.022 / 0.76	T3P8 (doublet)	0.017 / 0.76	C ₆ H ₄ CH ₃	0.018 / 0.75
IS11 (doublet)	0.023 / 0.74	T4P10 (doublet)	0.018 / 0.76	m-H(CH ₃)-C ₆ H ₃	0.051 / 0.76
IS12 (doublet)	0.022 / 0.73	T2/12 (doublet)	0.019 / 0.75	p-H(CH ₃)-C ₆ H ₃	0.048 / 0.76
IS13 (doublet)	0.021 / 0.75	T12P5 (doublet)	0.012 / 0.72	CH ₄ (singlet)	0.009 / 0.0
IS14 (doublet)	0.019 / 0.77	T10P8 (doublet)	0.019 / 0.73	NH ₃ (singlet)	0.009 / 0.0

4. Conclusion

In the present theoretical study, the potential energy surface for the $C_6H_5NH_2 + CH_3^*$ reaction has been figured out. The reactants, intermediate states, transition structures, and products of this reaction were optimized by using density functional theory M06-2X with the 6-311++G(3df,2p) basis set. Single-point energies for all species involved were also computed at the same level as shown in Fig. 1. The PES shows that the mechanism of the title reaction contains various channels leading to 14 intermediate states, 32 transition states, and 13 bimolecular products; in which 4 reaction paths proceed via H-abstraction processes resulting in P1 ($C_6H_5NH + CH_4$), P2 ($o-C_6H_4NH_2 + CH_4$), P3 ($m-C_6H_4NH_2 + CH_4$), and P4 ($p-C_6H_4NH_2 + CH_4$), the remaining channels occur via addition mechanisms leading to the P5 – P13 products. In terms of energy, the final bimolecular products (P1 – P4) created by the abstraction channels are more favorable than those formed by the addition channels. The most stable product, P1 ($C_6H_5NH + CH_4$), and the lowest channel in energy, $C_6H_5NH_2 + CH_3^* \rightarrow T0P1 \rightarrow P1$, were also identified in this study. The calculated present results will be further used for the kinetic calculations in the next study related to the title reaction. The computed energies together with the thermodynamic data of the species involved can be confidently used for modeling NH₂-related systems under atmospheric and combustion conditions.

Acknowledgments

This research is funded by Hanoi University of Science and Technology (HUST) under grant number T2021-PC-046.

References

- [1] G. Palmiotto, G. Pieraccini, G. Moneti, P. Dolara, Determination of the levels of aromatic amines in indoor and outdoor air in Italy, *Chemosphere* vol. 43, no. 3, pp. 355–361, Apr. 2001
[https://doi.org/10.1016/S0045-6535\(00\)00109-0](https://doi.org/10.1016/S0045-6535(00)00109-0).
- [2] M. F. Khan, X. Wu, B. S. Kaphalia, P. J. Boor, G. A. S. Ansari, Acute hematopoietic toxicity of aniline in rats, *Toxicol. Lett.*, vol. 92, no. 1, pp. 31–37, Jun. 1997
[https://doi.org/10.1016/S0378-4274\(97\)00032-5](https://doi.org/10.1016/S0378-4274(97)00032-5).
- [3] F. Shahrezaei, Y. Mansouri, A. A. L. Zinatizadeh, A. Akhbari, Photocatalytic degradation of aniline using TiO₂ nanoparticles in a vertical circulating photocatalytic reactor, *Int. J. Photoenergy*, vol. 2012, pp. 1–8, Sep. 2012
<https://doi.org/10.1155/2012/430638>.
- [4] J. Wang, H. Ma, P. J. Boor, V. M. S. Ramanujam, G. A. S. Ansaria, M. F. Khan, Up-regulation of heme oxygenase-1 in rat spleen after aniline exposure. *Free Radical Biology and Medicine*, vol. 48, no. 4, pp. 513–518, 2010
<https://doi.org/10.1016/j.freeradbiomed.2009.11.027>.
- [5] H. B. Xie, F. Ma, Y. Wang, N. He, Q. Yu, J. Chen, Quantum chemical study on Cl-initiated atmospheric degradation of monoethanolamine, *Environ. Sci. Technol.*, vol. 49, no. 22, pp. 13246–13255, Oct. 2015
<https://doi.org/10.1021/acs.est.5b03324>.
- [6] G. da Silva, Formation of nitrosamines and alkyldiazohydroxides in the gas phase: the $CH_3NH + NO$ reaction revisited, *Environ. Sci. Technol.*, vol. 47, no. 14, pp. 7766–7772, Jun. 2013
<https://doi.org/10.1021/es401591n>.
- [7] N. Dai, A. D. Shah, L. Hu, M. J. Plewa, B. McKague, W. A. Mitch, Measurement of nitrosamine and nitramine formation from NO_x reactions with amines during amine-based carbon dioxide capture for postcombustion carbon sequestration, *Environ. Sci. Technol.*, vol. 46, no. 17, pp. 9793–9801, Jul. 2012,
<https://doi.org/10.1021/es301867b>.
- [8] A. Mellouki, G. Le Bras, H. Sidebottom, Kinetics and mechanisms of the oxidation of oxygenated organic compounds in the gas phase, *Chem. Rev.*, vol. 103, no. 12, pp. 5077–5096, Oct. 2003
<https://doi.org/10.1021/cr020526x>.
- [9] R. Atkinson, Gas-phase tropospheric chemistry of organic compounds: a review. *Atmos. Environ.*, vol. 41, pp. 200–240, 2007
<https://doi.org/10.1016/j.atmosenv.2007.10.068>.
- [10] Y. Zhao, D. G. Truhlar, Density functional for spectroscopy: no long-range self-interaction error, good performance for rydberg and charge-transfer states, and better performance on average than B3LYP for ground states, *J. Phys. Chem. A*, vol. 110, no. 49, pp. 13126–13130, Nov. 2006
<https://doi.org/10.1021/jp066479k>.
- [11] G. E. Scuseria, C. L. Janssen, H. F. Schaefer III, An efficient reformulation of the closed-shell coupled cluster single and double excitation (CCSD) equations, *J. Chem. Phys.*, vol. 89, pp. 7382–7387, Aug. 1998,
<https://doi.org/10.1063/1.455269>.
- [12] C. Gonzalez, H. B. Schlegel, An improved algorithm for reaction path following. *J. Chem. Phys.*, vol. 90, no. 14, pp. 2154–2161, Feb. 1989
<https://doi.org/10.1063/1.456010>.
- [13] I. M. Alecu, J. Zheng, Y. Zhao, D. G. Truhlar, Computational thermochemistry: scale factor databases and scale factors for vibrational frequencies obtained from electronic model chemistries, *J. Chem. Theor. Comput.*, vol. 6, pp. 2872–2887, Aug. 2010.
- [14] M. J. Frisch, G. W. Trucks, H. B. Schlegel, G. E. Scuseria, M. A. Robb, J. R. Cheeseman, G. Scalmani, V. Barone, Petersson, *et al.*, Gaussian 16; Gaussian, Inc.: Wallingford CT, USA, 2016. Available: <https://gaussian.com/gaussian16>.
- [15] T. A. Klimova, V. V. Bochkarev, L. S. Soroka, Modeling of the aniline with nitrobenzene reaction by PM6 method, *Procedia Chemistry*, vol. 10, pp. 58 – 63, 2014,
<https://doi.org/10.1016/j.proche.2014.10.0>